Mahdi Shahparasti, Alvaro Luna, Joan Rocabert, Pau Bosch, Pedro Rodríguez. (2018) Realization of a 10 kW MES power to methane plant based on unified AC/DC converter. ECCE 2018: IEEE Energy Conversion Congress and Exposition: Portland, OR, USA: Sept. 23-27, 2018: IEEE, 2018. Pp. 3633-3640 Doi: 10.1109/ECCE.2018.8558013.

Mahdi Shahparasti, Alvaro Luna, Joan Rocabert, Pau Bosch, Pedro Rodríguez. (2018) Realization of a 10 kW MES power to methane plant based on unified AC/DC converter. ECCE 2018: IEEE Energy Conversion Congress and Exposition: Portland, OR, USA: Sept. 23-27, 2018: IEEE, 2018. Pp. 3633-3640 Doi: 10.1109/ECCE.2018.8558013.

Realization of a 10 kW MES Power to Methane Plant based on Unified AC/DC Converter

Mahdi Shahparasti[1], Alvaro Luna[1], Joan Rocabert[1], Pau Bosch[2] and Pedro Rodriguez[1,3]
1- Department of Electrical Engineering, Technical University of Catalonia , Barcelona, Spain
2- Leitat Technological Center, Barcelona, Spain
3- Department of Engineering, Loyola University, Seville, Spain
mshahparasti@yahoo.com, luna@ee.upc.edu, rocabert@ee.upc.edu, pbosch@leitat.org, prodriguez@ee.upc.edu.

Abstract— **This paper presents a galvanic isolated multi output AC/DC topology that is suitable for Microbial electrosynthesis (MES) based Power to Methane energy storage systems. The presented scheme utilizes a three phase back to back converters, a single-input and multiple-output three phase transformer, single diode rectifiers and buck converters that employ a proper interconnection between MES cells and the mains. The proposed topology merges all the required single phase AC/DC converters as a unified converter which reduces the overall system size and provides system integrity and overall controllability. The proposed control scheme allows to achieve the following desired goals:1) Simultaneous control of all cells; 2) Absorbing power from the grid and covert to methane when the electricity price goes down; 3) the power factor and the quality of grid current is under control; 4) Supplying MES cells at the optimal operating point. For verification of system performance, Real time simulation results that are obtained from a 10-kW MES energy storage are presented.**

Keywords— AC/DC power conversion, Microbial electrosynthesis (MES), Power-to- Methane plant.

I. Introduction

According to European mapping renewable energy pathways, renewable resources mainly solar and wind plants should provide 20 percent of EU's overall energy until 2020[1]. However, these resources are unstable and intermittent [2].To keep the grid supply and demand in balance, sometimes negative prices encourage producers to either shut power stations or else pay consumers to take the extra electricity off the network. Therefore, long-term and large capacity electricity storage is required, as well as reserve production capacity. The Power-to-Gas (P2G) especially Power-to- Methane technology might contribute to tackle this issue [3]. The P2G process links the power grid with the gas grid by converting surplus power into a grid-compatible gas. The position of P2G plants for handling high shares of renewable energies has been discussed [4, 5, 6].

A large number of later studies related Power-to-Methane have discussed about different technologies to convert wastewater and electricity to Methane and clean water using Microbial electrosynthesis (MES) cells [7-8].

Recent developments in MES technology solved several constraints, which were essential for the development of a MES-based P2G. These improvements make the MES more realistic and therefore requires the development of a process control system. In current technology, every MES cell should be supplied with DC voltage around 1V and consume around 20 mA. However, in power system studies, the MES is considered as a block box of storage with high capacity [9,10,11]. Therefore, the low capacity of MES cell is the big challenge for using this type of electricity storage in power system. As an example, a half million MES cells should be connected in series and parallel for achieving a 10kW storage.

In this paper, designing a 10kW controllable AC/DC converter to connect three-phase AC gird to MES storage is addressed. Supplying series MESs with equal voltage and tracking the maximum methane production should be performed by an AC/DC converter. The proposed converter supplies about a half million MESs. PWM rectifier is employed in the input stage to deliver fixed DC voltage to the output stage. The output stage is a unified three phase DC/DC converter which provides 210 separate DC voltages for blocks of MES cells.

This paper is organized as follows. In Sections II and III, MES modelling and the description of the proposed topology scheme are presented. In Section IV the simulation results that permits to analyze the performance of the proposed controller are presented. Likewise, the experimental performance is analyzed through real time simulator in Section V. Finally, the conclusions that arise from this work are presented in Section VI.

II. Modelling of MES and Voltage Balancing between Cells in a Stack

MES cells has been used to efficiently store electrical energy as a methane. Methane gas can be produced the cathode of MES, however, is not spontaneous [12 - 13]. The voltage produced by electrogenic bacteria on the anode is not sufficient to evolve methane gas. By applying a small voltage, methane gas can be produced using MESs at very high energy efficiencies evaluated in terms of just electrical energy alone (200-400%) or both electrical energy and substrate heat of combustion energy (82%)[14]. Therefore, MES cells produce

methane electrochemically through carbon dioxide reduction by the reaction

$$CO_2 + 8H^+ + 8e^- \rightarrow CH_4 + 2H_2O, \quad (1)$$

The produced methane can be transferred to natural gas distribution utility and there is not any difficulty related gas storage.

The characteristic curves of a typical MES include the relationship between the amount of produced methane and voltage across the cell, and the relationship between current and voltage across the cell are shown in Fig. 1[15-16-17]. As it can be seen from curves, the current and methane are almost zero for voltage below E_0, and they increase linearly after E_0.

According to the chemistry literature, the voltage applied to the cell E_{cell} have to be between E_{cell_min} and E_{cell_max}. Otherwise, the chemical behavior of the cell would be changed and unpredictable. The reported maximum voltage across cell (E_{cell_max}) is approximately 1.2 volts. To protect the cell, a Zener diode is commonly installed parallel with cell. Chemists also recommend that MES is not fed by voltage below than V_{cell_min}, MES change to open circuit state for voltage lower than V_{cell_min}.

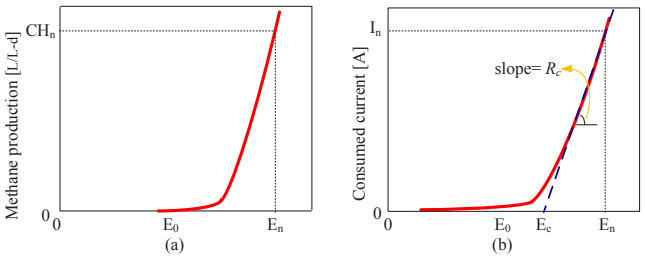

Fig. 1. Methane-Voltage and Current-Voltage curves for a typical MES cell.

The results shown in Fig. 1 are related to the steady state. In the transient state, MES cell behaves very slowly, and increasing current and methane from zero to nominal values, may require several hours to several days.

Until now, some research works have been proposed a passive model based on resistor, capacitor and DC source for Microbial Fuel Cells (MFCs) [18-19]. However, these models are not applicable for MES because 1) MES is a passive unidirectional element, but the previous models are bidirectional; 2) capacitor parallel with resistor cannot model correctly startup, and changing operation mode from open circuit mode and feeding with nominal voltage.

This paper proposes a new model for MES cell according to Fig. 2. This model becomes unidirectional with diode D_1 , R_c and E_c are chosen based slop of I-V curve as shown in Fig.1, and L_c is selected based on the time constant of MES cell. Diode D_2 is paralleled with L_c as a freewheeling diode to provide a path for release of stored energy while voltage drops to zero. This model with D2 is able to model the memory effect of MES cell while its working mode is changed.

The equivalent resistance in MES model can be expressed as follows:

$$R_c = \frac{E_n - E_c}{I_n}, \quad (2)$$

And, the equivalent inductor can be found from MES time constant τ_c:

$$L_c = \tau_c R_c = \tau_c \left(\frac{E_n - E_c}{I_n} \right), \quad (3)$$

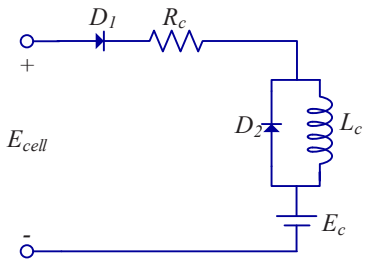

Fig. 2. Dynamic model of MES cell.

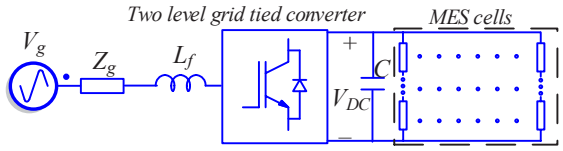

Fig. 3. Possible AC/DC topologies for supplying MES energy storage: single stage interlinking converter based on two level voltage source inverter.

III. Topology of Proposed AC/DC Converter

Fig.3-4 show different topologies for feeding MES cells as P2G energy storage.

In Fig. 3, a two-level three-phase voltage source converter is involved to link grid to MES system, where many cells are in series at DC link and V_{DC} are divided between them. The main drawback of this topology is that many cells have to be connected in series to obtain the desired voltage, therefore: 1) there is no grantee to divide DC link voltage equal between cells in series. Some passive components, such as resistors or capacitors, can be placed across groups of cells to satisfy equal voltage dividing. Energy dissipation in the case of using parallel resistance and slow response in the case of using capacitor parallel with cells can happen, 2) The impossibility of future development, 3) Lack of reliability due to connecting cells in series, 4) Unable to hot swap, 5) Low reliability, low protection against faults, weak expandability and modularity are the disadvantages of this topology, 6) Any faulty and open looped cell inhibits power consumption from the entire series-connected string of cells. If bypass diodes are used, then the fraction of energy that can be transferred to the cells but this branch does not operate in optimum working point, 7) It is very hard to identify the global maximum optimum point (MOP) for a branch with many series- connected cells because multiple local MPPs exist.

Fig. 4 depicts a typical topology to supply every MES block with individual AC/DC converter. Every AC/DC stage consists of diode rectifier, power factor correction (PFC) and DC/DC converter. This one does have the disadvantaged's two level voltage source converter but it suffers from using many semiconductors and passive components and also the poor input current quality. The other drawback of multi stage topology in

Fig. 4 is that it needs to a communication link between dc/dc converters and upper level control system, for controlling MES cells as an integrated power to methane plant.

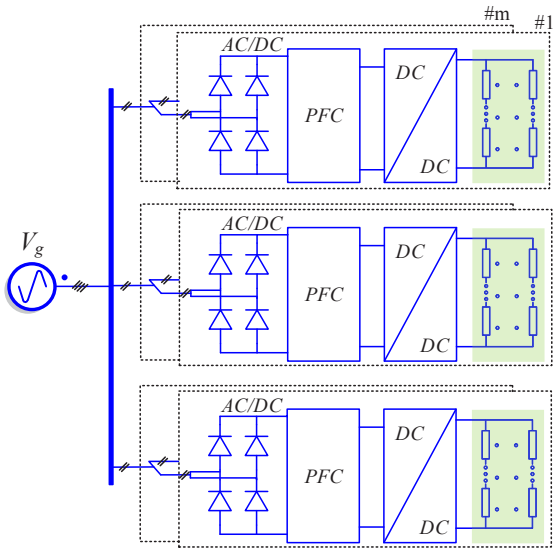

Fig. 4. Possible AC/DC topologies for supplying MES energy storage: multi stage interlinking converter based on diode rectifiers, power factor correction (PFC) stages and dc/dc converters.

Fig. 5 shows the block diagram of the proposed two-stage AC/DC topology, which able to control all MES cells simultaneously. It consisting of a PWM rectifier and multiple output DC/DC isolated converter. Around half million MES cells are divided to 210 blocks. Each MES block should be supplied with 24V and it consumes around 2A. The proposed converter feeds every block individually and independently.

A three-phase voltage source converter (VSI) is used as the rectifier in the input stage. In DC side, rectifier keeps the DC bus voltage under control and supplies the DC/DC converter with a fixed voltage. In AC side, it works in voltage supporting mode with controlling reactive power and drawing a sinusoidal current from the grid.

The main contribution of this paper is related to isolated DC/DC converter. A circuit diagram of the proposed output stage converter is shown in Fig. 5. This circuit consists of 3-phase IGBT based full-bridge inverter, unified multi-output three-phase transformer, 1-phase diode rectifiers and buck converters. The 3-phase inverter is switched with high frequency square wave modulation and with fixed duty cycle of 50%. Then, the three-phase pulsed voltage are applied to transformer. Each phase of transformer has *m* secondary output.

Hardware design

IV. Control Strategy of Proposed AC/DC Converter

The converter control strategy of input stage consists of two control loops (Fig. 5): current reference generator loop based

The detailed schematic of rectifier control scheme is shown in Fig. 6. The DC bus voltage V_{DC} is compared with its reference, and the error in voltage will be passed through a PI controller. The output of the PI controller will form the active power reference P^*. The reactive power reference Q^* is set zero to provide unity power factor. The current reference in the stationary reference frame $i^*_{\alpha\beta}$ is obtained from the following expression:

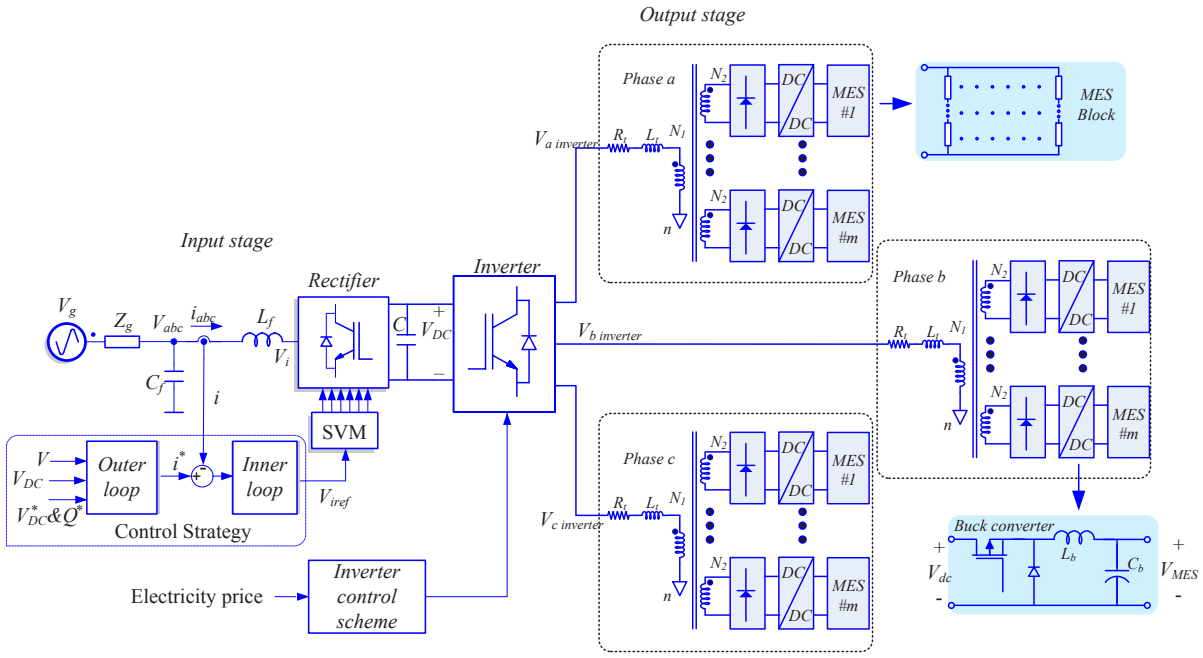

Fig. 5. Proposed the interlinking AC/DC converter for MES power to methane plant.

$$\begin{bmatrix} i_{\alpha+}^{*} \\ i_{\beta+}^{*} \end{bmatrix} = \frac{1.5}{v_{\alpha 1+}^{2}+v_{\beta 1+}^{2}} \begin{bmatrix} v_{\alpha 1+} & v_{\beta 1+} \\ v_{\beta 1+} & -v_{\alpha 1+} \end{bmatrix} \begin{bmatrix} P^{*} \\ Q^{*} \end{bmatrix} = T^{+} \begin{bmatrix} P^{*} \\ Q^{*} \end{bmatrix}, \quad (4)$$

where $v_{\alpha\beta 1}$ are the fundamental components of the grid voltage. The subscript + shows positive sequence. The Dual Second Order Generalized Integrator Frequency Locked Loop (DSOGI-FLL) is used for estimating the magnitude of the symmetrical components of the voltage at the PCC [20]. The PR controller is employed to track current reference with zero steady-state error and a fast dynamic response, which can be expressed as:

$$PR = K_p + \sum_{i=1,5,7} \frac{2\omega_c K_i s}{s^2 + 2\omega_c s + i^2\omega_o^2}, \quad (5)$$

where K_p, K_i, ω_o and ω_c are the proportional gain, the resonant gain, the resonant frequency and the resonant bandwidth, respectively. The tuning procedure for the PR controller parameters of grid-connected converter is the one described in [21].

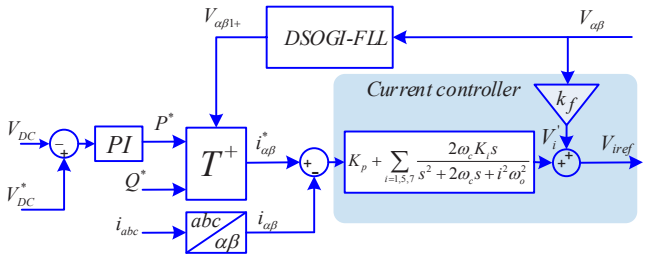

Fig. 6. Control scheme of input stage.

Rectifier always keeps DC bus voltage under control and fixes V_{DC} around nominal voltage (V_{DC} in this paper). For controlling the proposed topology, the inverter bridge in output stage is only switched in the case of reducing electricity price to convert electricity to methane. With switching of output inverter, the voltage is applied to the transformer and the single phase diode rectifiers are energized. The output voltage of diode rectifiers change around specific values and are not completely under control.

A DC/DC buck converter is used between diode rectifier and MES block. By this proposal, every MES block is fed individually. The block diagram of buck converter control scheme is shown in Fig. 7. Once the input voltage of buck converter reaches the threshold voltage ($V_{threshold}$ in Fig. 7), the buck converter will start to work and feed the MES at the optimal operating point (OOP).

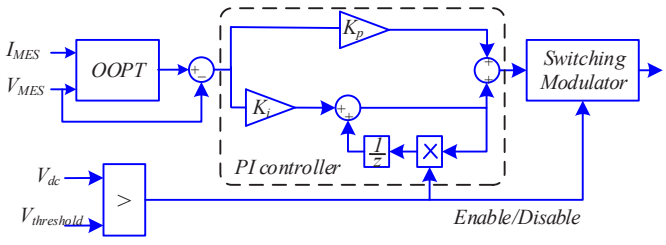

Fig. 7. Control scheme of buck converter in the output stage.

V. SIMULATION RESULTS

To verify the feasibility of the proposed two-stage AC/DC converter, time-domain studies were conducted in the MATLAB/SimPowerSystems™ environment. The parameters of input stage and output stage are given in Table 1.

In the simulation, it is supposed that the price of electricity reduces to zero between t=0.1s and t=0.25s. The obtained results are shown in Figs.6-8. Fig. 8 shows that the DC link voltage is always fixed around 700V. When the output stage turns off, the rectifier only absorbs active power for compensating losses including switching losses and conduction losses. Once the output stage starts to work, the voltage of DC link reduces and then the rectifier absorbs active power from grid to keep DC link voltage under control. The active and reactive powers waveforms illustrate that the average value of reactive power exchanged with the grid is around zero and the active power exchanged with the grid changes corresponding to the output power. The MES cells are modelled with a resistor and, they consume constant power during the simulation time.

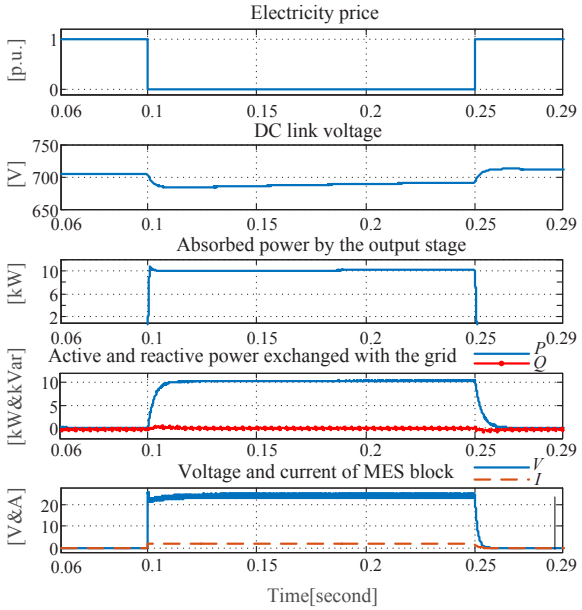

Fig. 8. Simulation results. From up: Electricity price in p.u., DC link voltage, the absorbed power by output stage, the active and reactive exchanged with the grid, voltage and current of a MES block.

Table 1 Proposed AC/DC parameters.

Input stage (Rectifier)		Output stage (DC/DC converter)	
Parameter	**Value**	**Parameter**	**Value**
Grid voltage	380V-50Hz	Transformer turn ratio (*N1:N2*)	4
Grid short circuit capacity (SCC)	10kA	Switching frequency of inverter	24kHz
LC filter inductor (L_f)	3.4mH	Output capacitor of single diode rectifiers	100μF
LC filter capacitor (C_f)	5 μF	Inductor of buck converter	80 μH
Switching frequency	10kHz	Capacitor of buck converter	1000 μF
DC link capacitor (C)	2200 μF	Buck converter switching frequency	50kHz

The waveforms of the absorbed current from the grid (rectifier current) is shown in Fig. 9, where it experiences an acceptable transient. Fig. 10 represents that THD (total harmonic distortions) of rectifier current is around 3.01% and it does not have low order harmonics such as the fifth and seventh harmonics.

The voltage and current of primary windings of the transformer are shown in Fig. 11, where they change with a fast transient response and without any DC offset. Also, Fig. 11 illustrates the output voltage of one of the diode rectifiers, it can be seen that it has been fixed around 31V with a ripple voltage 6V peak – peak. While according to Fig. 8, the output voltage of buck converter has been fixed at 24V.

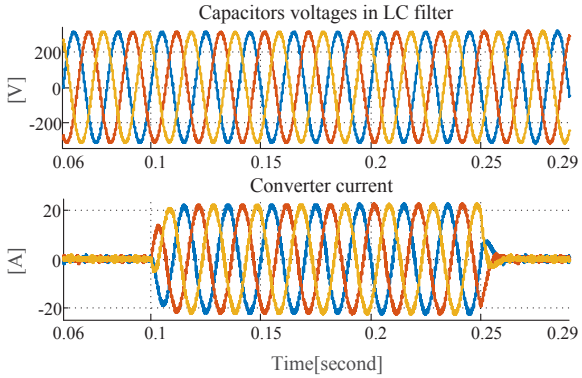

Fig. 9. Simulation results. From up: capacitors voltages of LC filter ("*V*" in Fig.1), converter current ("*i*" in Fig.1).

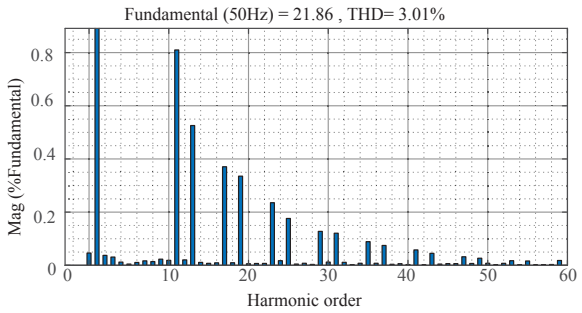

Fig. 10. Fourier spectrum of converter current.

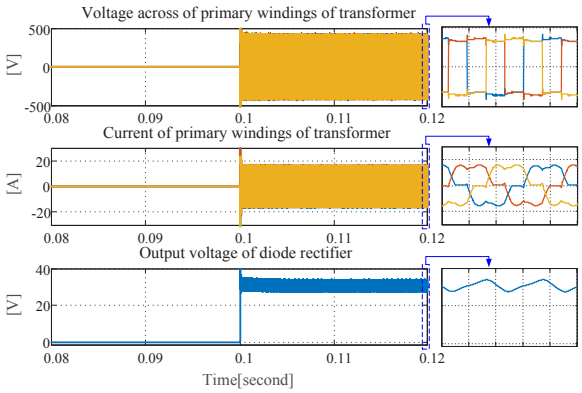

Fig. 11. Simulation results. From up: Voltage across of primary windings of transformer, Current of primary windings of transformer, Output voltage of diode rectifier.

VI. Real Time Simulator Results

This paper uses OPAL-RT-OP4510 as a real-time simulator in order to verify the performance of the proposed AC/DC topology. The real-time simulators are one of the best tools to evaluate the advances in power switching devices and power electronics converters impact different industries, applications, and emerging technologies. Equipped with the latest generation of Intel Xeon four-core processors and a powerful Xilinx Kintex7 FPGA, the OP4510 delivers raw simulation power for both CPU-based real-time simulation and sub-microsecond time step power electronic simulation. This feature makes it possible to couple high-speed FPGA-based models, such as power converters and electric drives, to slower electrical and mechanical systems on the CPU, providing even more detailed simulations. Fig. 12 and Fig. 13 show the schematic and setup of implementation of proposed system in OPAL-RT. The hardware part includes switches, diodes, electrical components and voltage and current sensors is implemented in FPGA . The hardware part runs fast with sample time 875ns second. The control system is implemented in CPU part and runs slow with sample time 10µs. Due to the increase in the switching frequency, the time step of the RT model should be much smaller than the converter's switching time step. Typical CPU-based RT simulation can only achieve a minimum time step of Ts ≥ 10 µs caused by the large bus latencies in a CPU. The OP4510 is also connected to an oscilloscope to monitor voltage, current and electrical power in real time. The values of voltages and currents are routed from the FPGA based model to the DAC channels directly.

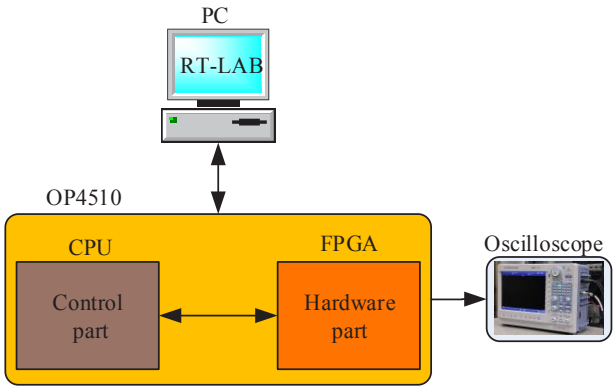

Fig. 12. Schematic of implementation of proposed system in OPAL-RT.

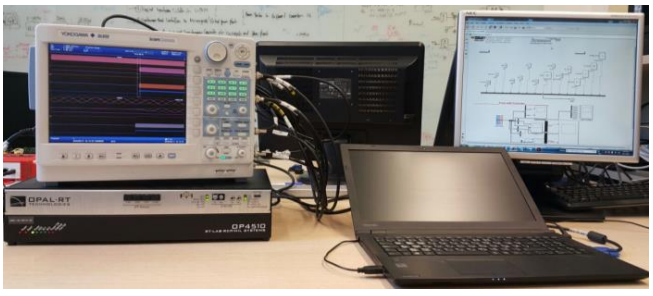

Fig. 13. Real time simulator setup.

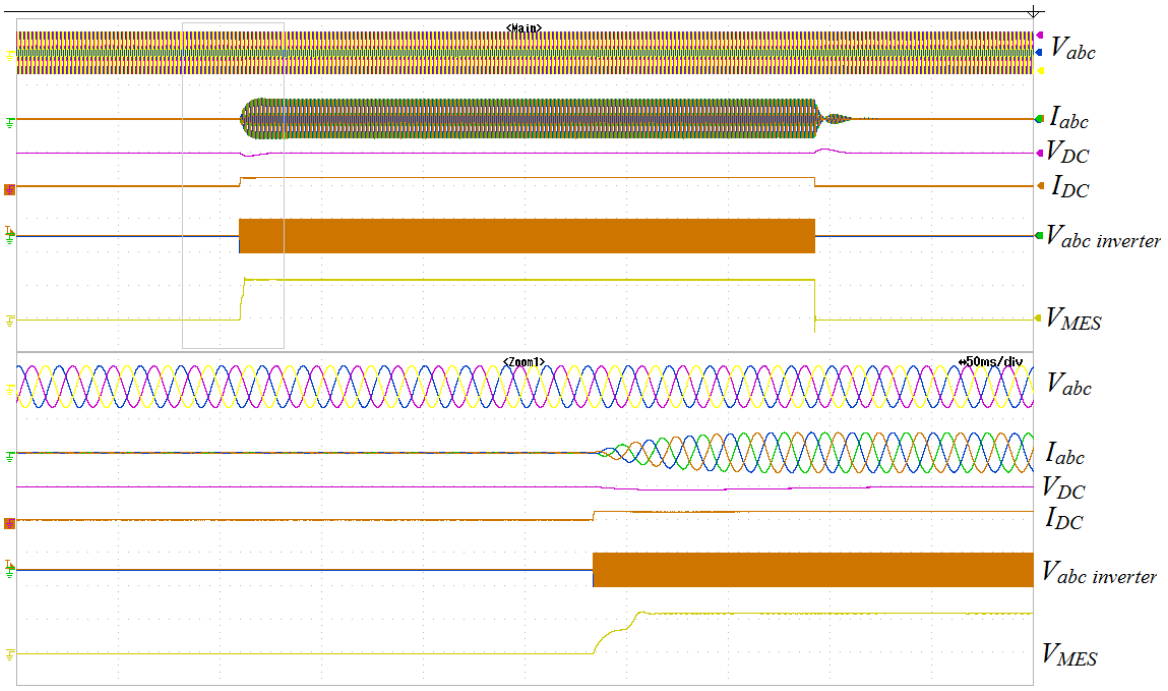

Fig. 14. Real time simulator results: turning on the proposed converter. From top: Grid voltage (V_{abc}, 1000V/div), Grid current (I_{abc}, 50A/div), DC link voltage (V_{DC}, 1000V/div), output voltages of inverter ($V_{abc\ inverter}$, 1000V/div), voltage of MES block (V_{MES}, 20V/div).

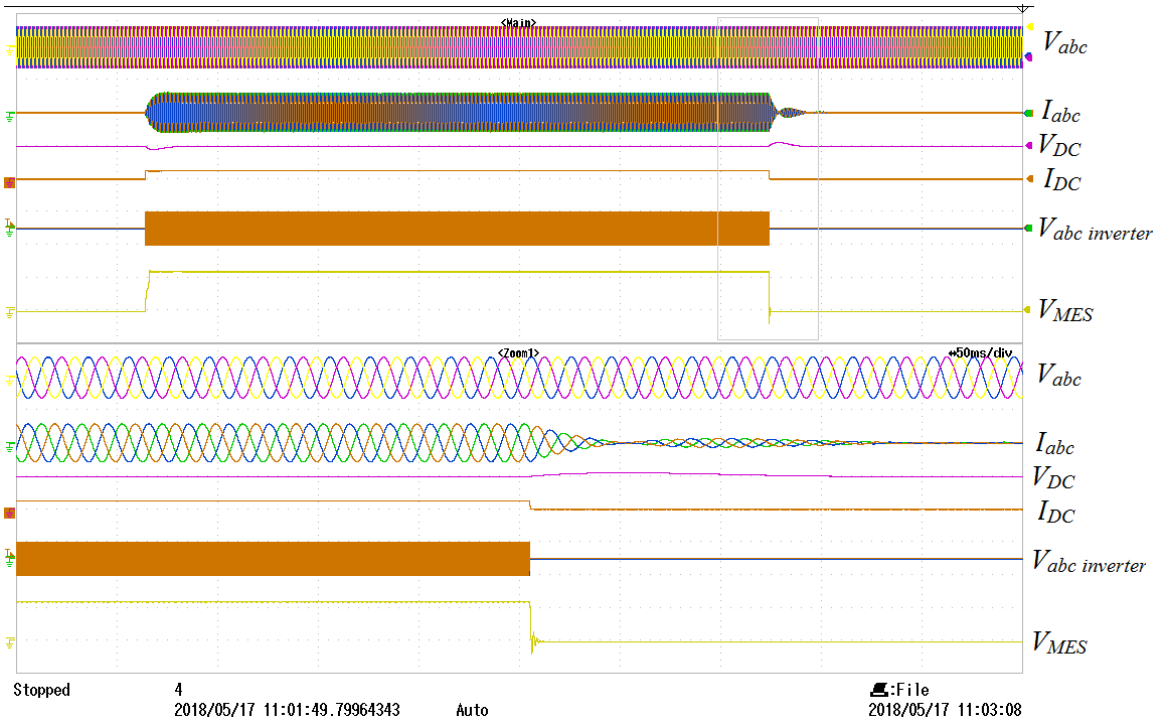

Fig. 15. Real time simulator results: turning off the proposed converter. From top: Grid voltage (V_{abc}, 1000V/div), Grid current (I_{abc}, 50A/div), DC link voltage (V_{DC}, 1000V/div), output voltages of inverter ($V_{abc\ inverter}$, 1000V/div), voltage of MES block (V_{MES}, 20V/div).

The parameters and other hardware data and control part are the same as the ones used in throughout the paper, listed also in Table I. Only, the switching frequency of inverter reduces from 24 kHz to 2 kHz due to the limited sample time of CPU in OPAL. Also, in MES block model, the values of R_c, L_c, E_n and E_c are set 4.8H, 4.8Ω, 24V and 14.4V, respectively.

In real time simulator, three capacitors are placed in series with the primary winding of transformer to remove the dc component of currents and to prevent transformer saturation.

Two cases have been selected in this validation stage, a startup of converter, where the price of electricity reduces to zero and a shutdown of converter in the case of incensement of electricity price. The results obtained in these tests are presented in Fig. 14 & Fig. 15 that show the transient performances of the two cases.

In start-up mode, 10 kW of active power are absorbed from the grid and the exchanged reactive power is zero. The dynamics of grid current is due to the inertia of the MES in the absorbing active power. As can be seen from the results, the DC bus voltage is regulated around its reference value (1000 V), and the DC current also changes rapidly at start-up. As it can be seen in the figure, the proposed PR controller offers a good response in front of sudden active power step, with minimal overshoot in current and short rise time. For the shutdown of converter, the results for input stage have the same transient response.

In output stage, the output voltages of inverter and MES block voltage are shown in Fig. 14 & Fig. 15. The results of this stage indicate that the inverter turns on and off immediately based electricity price, and subsequently the dc voltage appears at the input of the Buck converter. The Buck converter also feeds the MES block with a fixed voltage.

Zoomed view of the three phase inverter output voltage is shown in Fig. 16, the inverter is switched with square wave modulation method according to this figure.

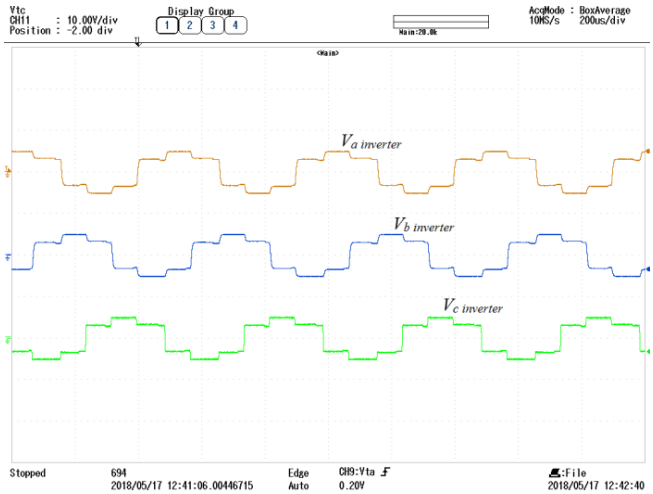

Fig. 16. Real time simulator results: output voltage of inverter, 1000V/div.

VII. Conclusions

The proposed two-stage AC/DC topology allows the supply of multiple MES blocks with desired voltage separately. This topology is suitable for power to methane plant. With the proposed control scheme, the topology can simultaneously supply MES blocks at the optimal operating point while drawing sinusoidal current (THD around 3%) with arbitrary power factor from the grid. The simulation results and also results of OPAL-RT real time simulator results confirm the effectiveness of the new topology.

Acknowledgment

The research leading to these results has received funding from the European Union's Horizon 2020 research and innovation programme under the Marie Skłodowska-Curie grant agreement No 712949 (TECNIOspring PLUS) and from the Agency for Business Competitiveness of the Government of Catalonia.

Also, this work has been supported by the Spanish Ministry of Economy and Competitiveness under the projects ENE2016-79493-R and ENE2017-88889-C2-1-R. Any opinions, findings and conclusions or recommendations expressed in this material are those of the authors and do not necessarily reflect those of the host institutions or funders.

References

[1] A. Zervos, C. Lins, L. Tesniere, Mapping Renewable Energy Pathways Towards 2020-EU ROADMAP, Brussels, Belgium, 2011.

[2] https://www.bloomberg.com/news/articles/2017-10-30/record-winds-in-germany-spur-free-electricity-at-weekend-chart

[3] A. ElMekawy, H. M. Hegab, G. Mohanakrishna, A. F. Elbaz, M. Bulut, and D. Pant, "Technological advances in CO2 conversion electro-biorefinery: A step toward commercialization," *Bioresour. Technol.*, vol. 215, pp. 357–370, 2016.

[4] M. Götz *et al.*, "Renewable Power-to-Gas: A technological and economic review," *Renew. Energy*, vol. 85, pp. 1371–1390, 2016.

[5] S. Clegg and P. Mancarella, "Integrated Modeling and Assessment of the Operational Impact of Power-to-Gas (P2G) on Electrical and Gas Transmission Networks," in *IEEE Transactions on Sustainable Energy*, vol. 6, no. 4, pp. 1234-1244, Oct. 2015.

[6] E. Pursiheimo, H. Holttinen and T. Koljonen, "Path toward 100% renewable energy future and feasibility of power-to-gas technology in Nordic countries," in *IET Renewable Power Generation*, vol. 11, no. 13, pp. 1695-1706, 11 15 2017.

[7] D. A. Jadhav, S. Ghosh Ray, and M. M. Ghangrekar, "Third generation in bio-electrochemical system research – A systematic review on mechanisms for recovery of valuable by-products from wastewater," *Renew. Sustain. Energy Rev.*, vol. 76, no. March, pp. 1022–1031, 2017.

[8] G. Kumar *et al.*, "A review on bio-electrochemical systems (BESs) for the syngas and value added biochemicals production," *Chemosphere*, vol. 177, pp. 84–92, 2017.

[9] D. Alkano and J. Scherpen, "Distributed supply coordination for Power-to-Gas facilities embedded in energy grids," in *IEEE Transactions on Smart Grid*, vol. PP, no. 99, pp. 1-1.

[10] S. Clegg and P. Mancarella, "Storing renewables in the gas network: modelling of power-to-gas seasonal storage flexibility in low-carbon power systems," in *IET Generation, Transmission & Distribution*, vol. 10, no. 3, pp. 566-575, 2 18 2016.

[11] C. He, L. Wu, T. Liu, and Z. Bie, "Robust Co-optimization Planning of Interdependent Electricity and Natural Gas Systems with a Joint N-1 and Probabilistic Reliability Criterion," *IEEE Trans. Power Syst.*, vol. 8950, no. c, 2017.

[12] D. Call, B. E. Logan," Hydrogen production in a single chamber microbial electrolysis cell (MEC) lacking a membrane," Environ. Sci. Technol, vol. 42, pp. 3401–3406, 2008,

[13] S. Cheng, D. Xing, D. F. Call, and B. E. Logan, "Direct Biological Conversion of Electrical Current into Methane by Electromethanogenesis," *Environ. Sci. Technol.*, vol. 43, no. 10, pp. 3953–3958, 2009.

[14] S. Cheng, B. E. Logan," Sustainable and efficient biohydrogen production via electrohydrogenesis," Proc. Natl. Acad. Sci., vol. 104, pp. 18871–18873, 2007

[15] S. Cheng *et al.*, "Direct Biological Conversion of Electrical Current into Methane by Electromethanogenesis Direct Biological Conversion of Electrical Current into Methane by Electromethanogenesis," vol. 43, no. 10, pp. 3953–3958, 2009.

[16] M. C. A. A. Van Eerten-Jansen, A. Ter Heijne, C. J. N. Buisman, and H. V. M. Hamelers, "Microbial electrolysis cells for production of methane from CO2: long-term performance and perspectives," *Int. J. energy Res.*, vol. 31, no. August 2007, pp. 135–147, 2007.

[17] G. Zhen, X. Lu, G. Kumar, P. Bakonyi, K. Xu, and Y. Zhao, "Microbial electrolysis cell platform for simultaneous waste biorefinery and clean electrofuels generation: Current situation, challenges and future perspectives," *Prog. Energy Combust. Sci.*, vol. 63, pp. 119–145, 2017.

[18] D. Recio-garrido, M. Perrier, and B. Tartakovsky, "Modeling, optimization and control of bioelectrochemical systems," *Chem. Eng. J.*, vol. 289, pp. 180–190, 2015.

[19] S. Carreon-Bautista, C. Erbay, A. Han and E. Sánchez-Sinencio, "Power Management System With Integrated Maximum Power Extraction Algorithm for Microbial Fuel Cells," in *IEEE Transactions on Energy Conversion*, vol. 30, no. 1, pp. 262-272, March 2015

[20] P. Rodríguez, A. Luna, I. Candela, R. Mujal, R. Teodorescu, and F. Blaabjerg, "Multiresonant frequency-locked loop for grid synchronization of power converters under distorted grid conditions," *IEEE Trans. Ind. Electron.*, vol. 58, no. 1, pp. 127–138, 2011.

[21] M. Shahparasti, P. Catalán, J. I. Candela, A. Luna, and P. Rodríguez, "Advanced control of a high power converter connected to a weak grid," *IEEE Energy Convers. Congr. Expo. (ECCE), Milwaukee*, pp. 1–7, 2016.